



Activation process of Pd/Al₂O₃ catalysts for CH₄ combustion by reduction/oxidation cycles in CH₄-containing atmosphere

Paola Castellazzi^a, Gianpiero Groppi^{a,*}, Pio Forzatti^a, Elisabetta Finocchio^b, Guido Busca^b

^a Laboratory of Catalysis and Catalytic Processes, Dipartimento di Energia, Politecnico di Milano, Piazza Leonardo da Vinci 32, 20133 Milano, Italy

^b Dipartimento di Ingegneria Chimica e di Processo, Facoltà di Ingegneria, Università di Genova P.le Kennedy 1, 16126 Genova, Italy

ARTICLE INFO

Article history:

Received 8 February 2010

Revised 23 July 2010

Accepted 29 July 2010

Available online 15 September 2010

Keywords:

CH₄ combustion

Palladium catalysts

Natural gas vehicles

Pd-support interactions

ABSTRACT

In this work, the effect of a conditioning process, consisting of several alternated CH₄-lean combustion/CH₄-reducing pulses at 350 °C, was investigated over Pd/Al₂O₃ catalysts with different Pd loadings (1, 2 and 4 w/w%) prepared from Cl-free precursors. Such a treatment resulted in a one order of magnitude activity enhancement and in the achievement of stable catalytic performances in all the investigated systems. The activity enhancement was associated with an increase in PdO reducibility, as revealed by the comparison of CH₄-TPR profiles before and after the conditioning process. Characterization studies showed that negligible or minor (for the 1% w/w Pd sample) modifications of Pd dispersion occurred upon conditioning, thus ruling out a significant effect of particle size variations on the observed activity enhancement. TPR, FT-IR and XRD measurements showed that palladium is completely oxidized upon conditioning, PdO is less crystalline than in the fresh catalyst likely due to the low oxidation temperature in the conditioning cycles but high activity was retained upon re-crystallization of PdO at 600 °C. FT-IR characterization revealed that conditioning results in a weakening of Pd-support interactions, which possibly originated from the interaction of the acidic Pd precursor with basic hydroxyls of the alumina surface, which acts as germination center during the impregnation step. Such a weakening of Pd-support interactions is likely responsible for the observed activity/reducibility enhancement.

© 2010 Elsevier Inc. All rights reserved.

1. Introduction

Natural gas vehicles (NGVs) operated under lean burn conditions guarantee a higher combustion efficiency and minimize the typical products of incomplete combustion, such as soot, CO and volatile organic compounds (VOCs) in addition to CO₂ emissions [1,2]. On the other hand, CH₄ is a strong green house gas, with a global warming potential higher than that of the CO₂; thus, large emissions of CH₄ would represent an environmental problem. Catalytic combustion of methane represents a promising way to reduce unburned CH₄ from the NGVs emissions. In the exhaust conditions, i.e. low temperatures, low CH₄ concentrations and presence of varying concentrations of O₂, H₂O, CO₂, NO_x and SO_x [3], the superiority of Pd-based catalysts has been widely recognized and their performances have been extensively investigated [4]. Nevertheless, many factors controlling the CH₄ combustion activity of Pd-supported catalysts are still debated [1–4].

Several studies [5–13] mentioned large enhancements of the activity of Pd-supported catalysts with time on stream before achieving a steady state behavior. It is now widely admitted that some activation periods reported in the early studies [5–8] are

related to the slow removal from the catalyst of residual chlorine, coming from Pd salt precursors or from the support impurities [14–16], which has a strong deactivating effect on Pd catalysts [14,17]. However, chlorine removal is not the only cause of activity enhancement since time-dependent activation phenomena were reported also for chlorine-free catalysts. Garbowski et al. [9] correlated the increase in the catalytic activity of Pd/Al₂O₃ catalysts, observed after reaction tests at 600 °C under both fuel-rich and fuel-lean CH₄/O₂ mixture, to a surface reconstruction of palladium particles under the influence of the reactants; on the basis of spectroscopic techniques, they observed that the Pd(1 1 1) planes, prevailing on the fresh catalysts, disappear after reaction while Pd(1 0 0) and Pd(1 1 0) planes form.

Some authors [18,19] attributed the activation of palladium catalysts to the roughening of the surface occurring during reaction conditions. Others reported that CH₄ combustion activity is influenced by palladium particle size [1–5,20]; a high dispersion of palladium oxide, giving an intimate contact with the support, stabilizes PdO against decomposition and reduction leading to a lower specific activity according to a Mars–Van Krevelen redox mechanism for CH₄ oxidation [20].

As a whole, the effect of the presence of contaminants (chlorine), Pd reconstruction, metal–support interactions and Pd particle size may be responsible for the wide variation in TOFs

* Corresponding author. Fax: +39 02 2399 3318.

E-mail address: gianpiero.groppi@polimi.it (G. Groppi).

reported in the literature [5,20–25] for CH₄ combustion, spanning more than two orders of magnitude [24].

Such a lack of quantitative understanding of the factors controlling CH₄ combustion activity of palladium catalysts can bias investigations into the role of preparation variables such as the choice of the support. Besides, from a practical point of view, uncontrolled detrimental effects can result in relatively poor CH₄ conversion performances of palladium catalysts.

In this respect, in previous works [3,26], we have mentioned alternated reduction/re-oxidation cycles under CH₄-containing atmosphere as an effective activation method to obtain high conversion performances over conventional Pd/Al₂O₃ catalysts prepared by a simple dry impregnation technique. Such a conditioning treatment resulted in a marked enhancement of the catalytic activity of the fresh samples, up to the achievement of steady state behavior; the final TOFs reported in Ref. [3] are comparable to the highest TOF values reported in the literature by Ribeiro et al. [24].

In this work, we investigated in detail the conditioning process of Pd/Al₂O₃ catalysts, consisting of alternated CH₄-lean combustion/CH₄-reducing pulses at 350 °C. The scope was to gain insight into the modifications responsible for the activity enhancement, thus providing a rational to develop practical activation methods. Three catalytic systems having different Pd loadings (1, 2 and 4% wt) were prepared starting from Cl-free Pd precursors. The activity evolution during the conditioning process was carefully monitored, and the different samples were characterized before and after the conditioning process by H₂ chemisorption, CH₄-TPR, XRD and FT-IR techniques.

2. Experimental

2.1. Catalysts preparation

Palladium supported on alumina catalysts were prepared starting from a commercial alumina (Sasol Puralox SBA140) calcined at 950 °C for 10 h in air in order to stabilize structural and morphological properties. A θ -Al₂O₃ (with traces of γ) phase was obtained with a specific surface area of 100 m²/g and a pore volume of 0.49 cm³/g. Different palladium loadings (1, 2 and 4 w/w%) were added by a dry impregnation technique, starting from an aqueous solution containing the Pd(NO₃)₂ precursor (Alfa Aesar) in appropriate amounts. The prepared catalysts were dried at 110 °C for 2 h and treated at 600 °C for 10 h in air before any testing.

2.2. Catalysts characterization

The experimental Pd loadings were determined by atomic absorption analysis (AAS) on a Varian AA110 apparatus. Palladium dispersion was estimated by H₂ chemisorption measurements on a Micromeritics AutoChemII instrument: the catalysts were first reduced in 5% H₂ in Ar stream at 500 °C for 1 h; then, after a 2-h Ar purge at 500 °C, the temperature was decreased to 70 °C and 5% H₂ in Ar pulses (0.961 ml) were injected at regular interval times. A H/Pd = 1/1 stoichiometry was assumed. Palladium dispersion was estimated for both the *fresh* samples, i.e. the calcined at 600 °C in air sample before any testing, and the catalysts underwent repeated redox cycles at 350 °C, according to the procedure illustrated in the next section, hereafter called *conditioned* catalysts.

The mean Pd particle diameters d_p (nm) were estimated from dispersion data using the following expression derived from hemispherical particles [22]:

$$d_p = \frac{6 \cdot C_a \cdot PM \times 10^9}{\rho \cdot D \cdot N_{av}}$$

with C_a concentration of surface metal atoms, equal to 1.27×10^{19} atoms/m², PM Pd atomic mass, ρ Pd volumetric mass equal to 12.02×10^6 g/m³, D metal dispersion and N_{av} Avogadro number [22].

XRD patterns were recorded on a Philips (PW 1050/70) powder diffractometer using a vertical goniometer and the Cu K α radiation ($\lambda_{K\alpha} = 0.1518$ nm). XRD patterns were collected on the fresh and conditioned 2% Pd/Al₂O₃ sample and over the conditioned sample subsequently exposed to dry lean reaction conditions (0.5% CH₄, 4% O₂, N₂ at balance) at 600 °C for 5 h (called conditioned-600).

FT-IR experiments were performed on the fresh 2% Pd/Al₂O₃ catalyst and on the same conditioned sample. For FT-IR studies, pure alumina support and 2% Pd on alumina-powdered catalysts were pressed in self-supporting disks (average weight 20 mg), outgassed at 500 °C, or reduced in pure hydrogen (400 torr) and outgassed at 500 °C directly in the IR cell connected to a gas manipulation apparatus. CO adsorption was performed at liquid nitrogen temperature (around 10 torr CO gas, “full coverage”). FT-IR spectra were recorded, outgassing at increasing temperature in the range –130 °C to room temperature at decreasing CO coverage.

2.3. Catalytic activity test

Catalytic activity tests were performed in a fixed-bed quartz microreactor (ID = 7 mm) placed inside an electrically heated furnace. The reactor was loaded with 60 mg of fine catalytic powder (74–105 μ m) diluted with quartz of the same particle size, with a different dilution ratio depending on Pd loadings (Pd/quartz equal to 1 for the 1% and 2% Pd catalysts and to 3 for the 4% Pd sample in order to minimize temperature gradients). The catalyst temperature was monitored using a K-type thermocouple located in the center of the catalytic bed. Composition of the reactants and products at the outlet of the reactor was monitored by a mass spectrometer with a quadrupole detector (Balzers QMS 422). Periodical GC analyses were performed with a HP6890 Systems in order to calibrate CH₄, CO₂ and O₂ MS signals and to more precisely quantify CH₄ conversion.

The following experiments were performed on the prepared samples:

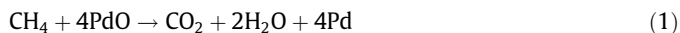
- alternated redox cycles under CH₄-containing atmosphere at constant temperature (350 °C): the catalysts were operated for 30 min under CH₄-lean combustion conditions (0.5% CH₄, 4% O₂, 1% H₂O, 2% N₂ and He at balance, GHSV = 150,000 Ncm³/g_{cat}/h, atmospheric pressure); then, after a 30–40 s inert purge (5% N₂ in He), performed to allow the desorption of species from the catalytic surface, the reaction atmosphere was switched to rich conditions, exposing the catalysts for 2 min to a CH₄-reducing stream (0.5% CH₄, 1% H₂O, He at balance, GHSV = 150,000 Ncm³/g_{cat}/h, atmospheric pressure); after another purge, the lean conditions were restored. The procedure was repeated several times during the conditioning process.
- CH₄-TPR: the catalysts were exposed to a reducing stream (0.5% CH₄, 1% H₂O, He at balance, GHSV = 150,000 Ncm³/g_{cat}/h, atmospheric pressure), and the temperature was raised up to 500 °C and down to RT at 15 °C/min.

3. Results

3.1. Conditioning process

Fig. 1 shows the time evolution of CH₄, CO₂ (ppm) and H₂ (a.u.) outlet concentrations during one typical lean combustion/

CH₄-reducing pulse/lean combustion cycle at 350 °C for the three investigated Pd/Al₂O₃ catalysts; the intervals between dotted lines correspond to the inert purge periods, performed to separate the oxidizing and the reducing atmosphere. For each catalyst, when switching from the lean conditions to the CH₄-reducing pulse, the CH₄ outlet concentration exhibited a delay associated with a sharp consumption peak followed by the achievement of a plateau; correspondingly, the CO₂ outlet concentration showed a sharp release peak followed by a similar plateau. CO₂ release and CH₄ consumption associated with the observed peaks were always well in agreement with the reduction in the entire amounts of palladium present in each catalyst, according to the following stoichiometry:



Only after the initial peak, in correspondence with the plateau in the CH₄ and CO₂ concentration profiles, CO (not reported in the fig-

ure) and H₂ were observed, probably associated with the onset of the steam reforming and water–gas shift reactions on metallic palladium.

Upon restoring the lean conditions after reduction, all the catalysts exhibit a gradual increase in CO₂ production corresponding to an increase in CH₄ consumption, up to the achievement of a minimum for CH₄ and a maximum for CO₂ concentrations; as we have shown in our previous works [3,26], this reactivation trend is associated with the re-oxidation of the metallic palladium formed during the previous reducing pulse.

While the concentration trends observed during the reducing pulses kept practically unaltered, a marked evolution of the catalyst performance under lean conditions progressively occurred during the conditioning process. In Fig. 2, the trends of conversion vs. time on stream observed upon switching to lean conditions after a given number of reduction/re-oxidation cycles are reported. For all the samples, the initial activity of the fresh catalysts, which did not undergo any reduction treatment, was very low and a slowly decreasing conversion trend was always observed, evidencing that no activation occurred under lean reaction conditions in the absence of any pre-reduction treatment. The deactivation trend of the fresh 1% Pd sample seems more pronounced with respect to the 2% and 4% Pd catalysts. However, it is a very low conversion data, subjected to major experimental uncertainties.

Upon the first reduction cycle, the typical reactivation trend associated with palladium re-oxidation was observed. In all the catalysts, a CH₄ conversion level higher than that of the fresh materials was observed upon reactivation. As shown in Fig. 2, such an activity enhancement further increased upon a number of reduction/re-oxidation cycles, and a stable behavior was finally achieved only after many cycles, characterized by completely reproducible conversion trends which were maintained during several additional cycles.

To better focus the extent of the conversion performance enhancement associated with alternated reduction/oxidation cycles on the catalytic activity, the CH₄ conversion values determined by GC measurements after 10 min of exposure of the investigated Pd/Al₂O₃ samples to the lean conditions are reported in Fig. 3 as a function of the number of cycles. The 1% Pd catalyst, exhibiting an initial CH₄ conversion of about 5%, showed a progressive increase in activity cycle after cycle, up to the stabilization in correspondence with a conversion level of about the 30% after 11–13 cycles. In the case of the 2% and 4% Pd samples, the activation trends were similar but slightly faster than those observed for the 1% Pd catalyst; CH₄ conversion increased from an initial level of 10% and 25%, for the 2% and 4% Pd samples, respectively, up to a final stable level of about 70% for both the catalysts, achieved after 9–10 cycles and after 7–8 cycles respectively.

Palladium dispersion was measured before and after the conditioning process by H₂ chemisorption. The obtained values are reported in Table 1. The fresh 1% Pd catalyst was characterized by the highest dispersion value (66%), while the fresh 2% and 4% Pd samples showed similarly lower dispersions (20% and 22%, respectively); after the conditioning process, palladium dispersion slightly decreased, from 66% to 48%, only in the case of the 1% Pd catalyst, whereas it remained substantially unchanged for the 2% and 4% Pd ones (21% and 19%, respectively).

To quantify the intrinsic activity enhancement associated with the conditioning process, TOF values of fresh and conditioned catalysts were calculated based on the integral conversion data reported in Fig. 3, using the metal surface atoms estimated from dispersion data as a reference evaluation of the number of the active sites. In such calculations, an isothermal (350 °C), pseudo-homogeneous, plug flow behavior of the reactor was assumed. Rate constant referred to the unit catalyst weight was obtained by the analytical solution of the differential mass balance derived for a

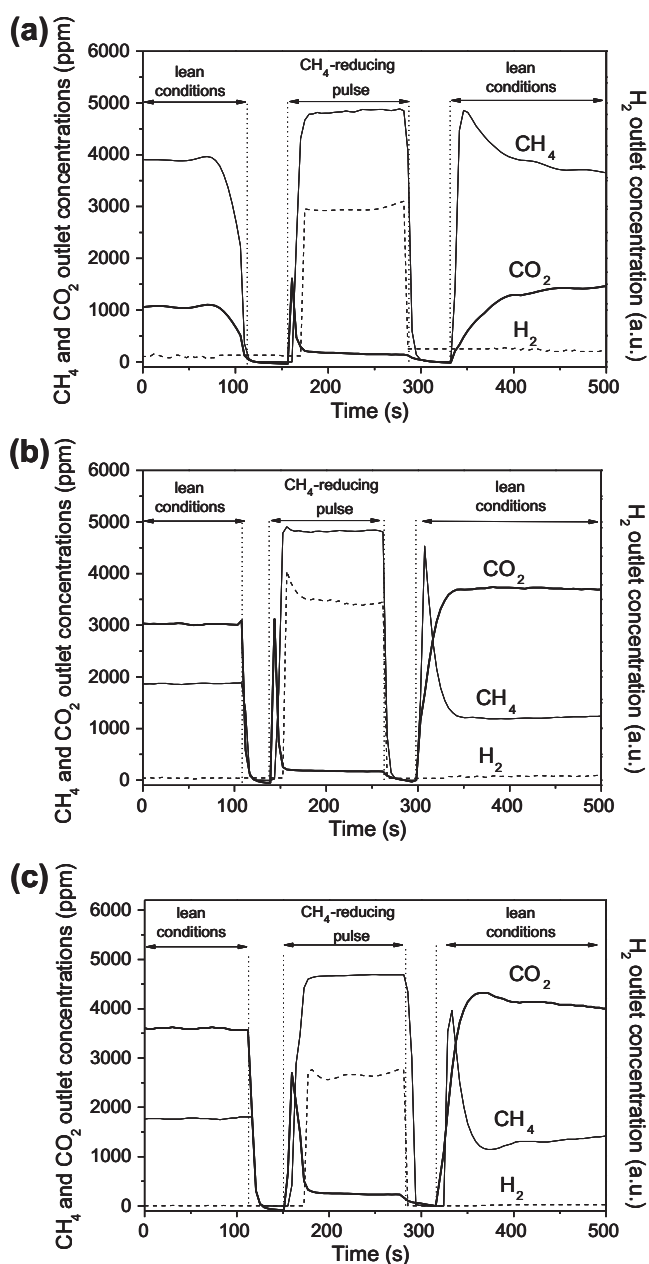


Fig. 1. Time evolution of CH₄ and CO₂ outlet concentrations (ppm) and of H₂ signal (arbitrary units) during lean combustion conditions alternated to a CH₄-reducing pulse at 350 °C for the 1% Pd/Al₂O₃ (a), 2% Pd/Al₂O₃ (b) and 4% Pd/Al₂O₃ (c) catalysts.

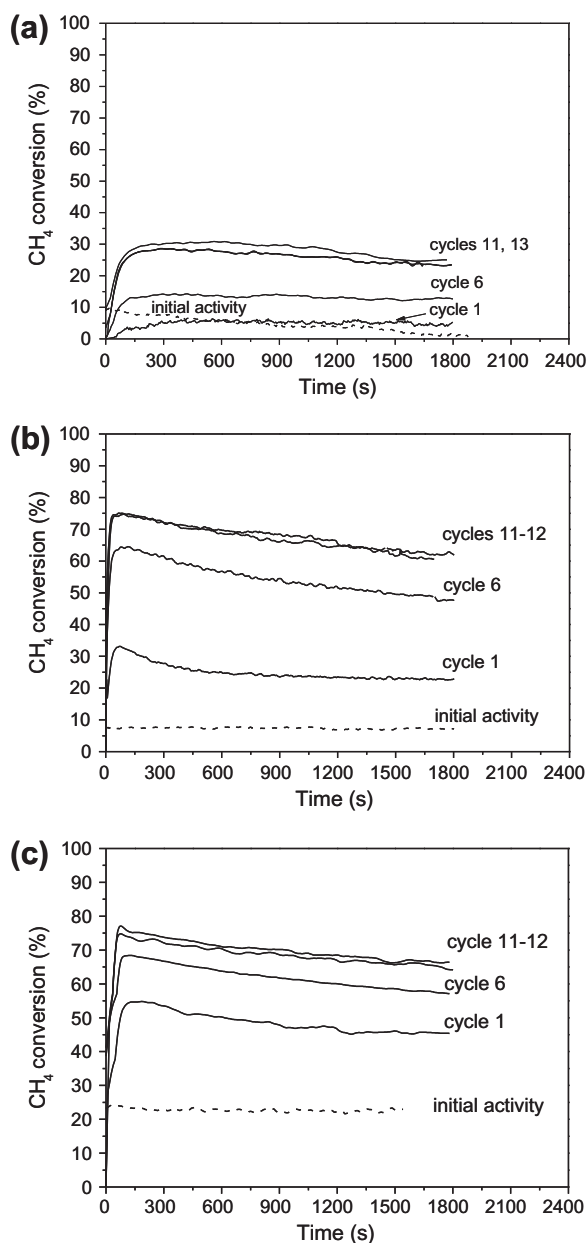


Fig. 2. CH₄-conversion trends upon switching to lean combustion conditions at 350 °C after a given number of reduction/oxidation cycles for the 1% Pd/Al₂O₃ (a), 2% Pd/Al₂O₃ (b) and 4% Pd/Al₂O₃ (c) catalysts.

power law CH₄ combustion kinetics with 1, –1 and 0 reaction-order dependences on CH₄, H₂O and O₂ concentrations, respectively, which were assumed according to many literature indications [21,27–29]. TOFs were finally evaluated at the following conditions: $P_{\text{CH}_4} = 0.5$ kPa, $P_{\text{H}_2\text{O}} = 1.1$ kPa, $T = 350$ °C, using Pd load and dispersion data. In the case of the fresh samples, TOFs of 5.6×10^{-3} , 1.7×10^{-2} and $3.5 \times 10^{-2} \text{ s}^{-1}$ were calculated, respectively, for the 1%, 2% and 4% Pd samples; the same systems, after conditioning process, exhibit TOFs of 7.3×10^{-2} , 3.6×10^{-1} and $2.3 \times 10^{-1} \text{ s}^{-1}$, respectively, corresponding to an intrinsic activity enhancement of about 10–20 times. Although such estimations may suffer from some uncertainties associated with approximations on thermal and flow behavior of the reaction and with minor deviations from the adopted reaction orders, the results clearly indicate that one order of magnitude activation occurred in all the investigated catalysts upon conditioning.

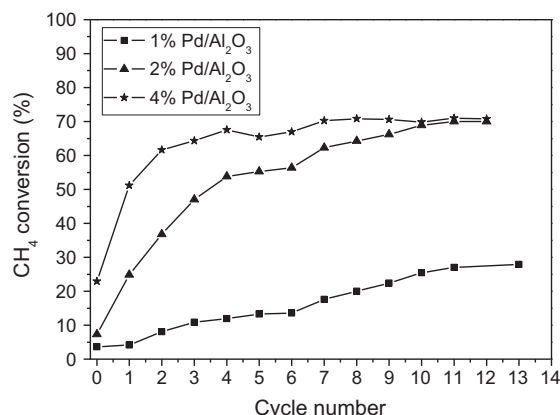


Fig. 3. CH₄ conversion after 10 min of exposure to the lean conditions at 350 °C as a function of the redox cycles number for the 1%, 2% and 4% Pd/Al₂O₃ catalysts.

3.2. Reducibility

Reducibility of fresh and conditioned catalysts was investigated by means of CH₄-TPR. In all the samples, CH₄ conversion during the TPR profiles (Fig. 4) shows a peak, accompanied by CO₂ and H₂O release, associated with the PdO reduction according to the stoichiometry of reaction (1), followed by a gradual increase in the temperature, associated with the release of CO and H₂ in addition to CO₂ and H₂O, likely related to the steam reforming and water-gas shifts reactions. The quantification of CH₄ consumption and CO₂ release associated with the reduction peaks indicates that for the three investigated catalysts, both fresh and conditioned, the whole amount of palladium in the samples is present as PdO. In the case of the fresh 1% Pd sample, PdO reduction starts at 330 °C, while for both the fresh 2% and 4% Pd samples, PdO reduction begins at lower temperature (300 °C). After the conditioning process, the onset of the PdO reduction reaction shifts to lower temperatures: 300 °C for the 1% Pd catalyst and about 280–290 °C for the 2% and 4% Pd samples.

3.3. Characterization results

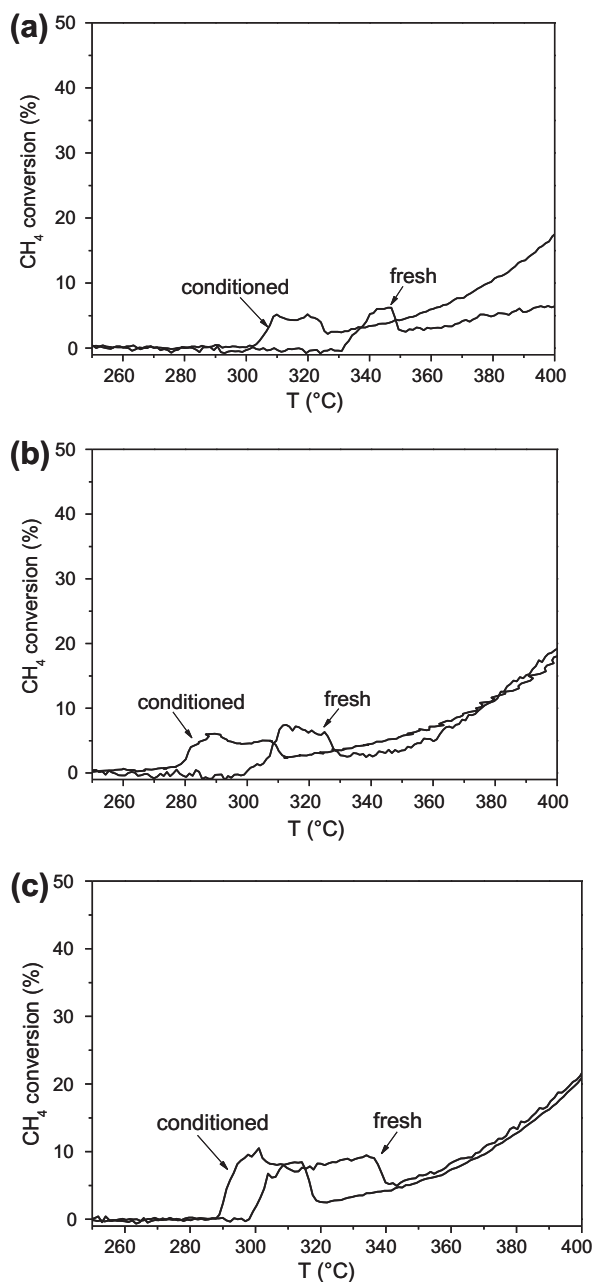
In order to obtain further insight into modifications associated with the conditioning treatment, the reference 2% Pd catalyst was characterized by means of XRD and FT-IR techniques.

3.3.1. XRD

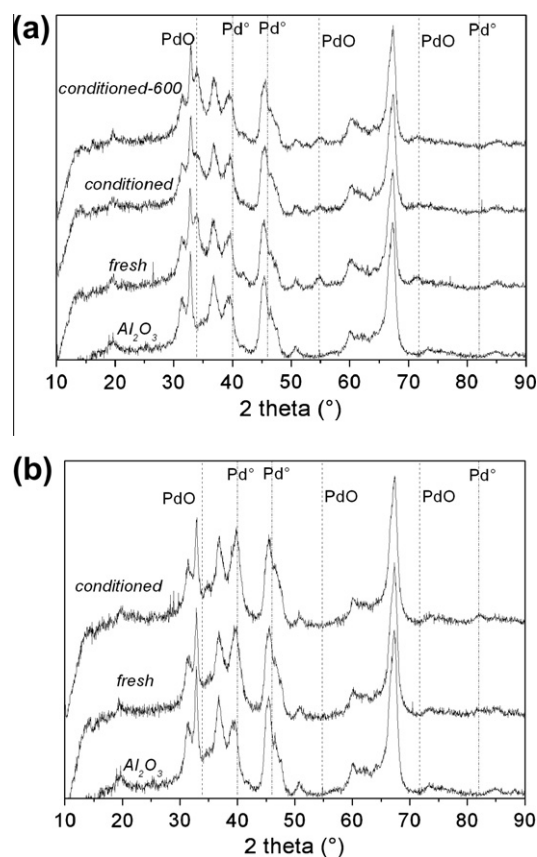
Fig. 5a shows the XRD spectra of the following 2% Pd samples: fresh; conditioned; exposed to dry lean combustion conditions at 600 °C after conditioning. In all the cases, only PdO reflections are detected in addition to the alumina ones, while no metal Pd⁰ patterns are present. Comparing the spectra of the fresh and conditioned samples, the broader peaks of PdO in the conditioned sample (see e.g. the peak at $2\theta = 34^\circ$) may suggest the formation of a poorly crystalline PdO. In fact, the conditioning process involves the PdO reduction during a CH₄-pulse and PdO reformation during the lean combustion conditions at 350 °C, a significantly lower temperature than that adopted in the preparation procedure (600 °C in air), which may justify the better crystallization of PdO in the fresh sample. To clarify this point, the conditioned sample was further treated under dry reaction feed conditions at 600 °C. The XRD of the conditioned-600 shows PdO reflections very similar for height, width and shape to those of the fresh system, confirming the formation of a more crystallized PdO phase upon oxidizing treatments at 600 °C. The estimation of PdO particle size on the bases of the Scherrer equation results in PdO crystallites of about

Table 1Main characteristics of fresh and conditioned 1%, 2% and 4% Pd/Al₂O₃ catalysts.

Nominal Pd loadings (%)	AAS Pd loadings (%)	H ₂ chemisorption dispersion (%)		TOF (s ⁻¹) ^b	
		Fresh	Conditioned	Fresh	Conditioned
1	1.01	66 (1–2 nm) ^a	48 (2–3 nm) ^a	5.6×10^{-3}	7.1×10^{-2}
2	2.14	20 (6 nm) ^a	21 (6 nm) ^a	1.7×10^{-2}	3.6×10^{-1}
4	3.94	22 (5 nm) ^a	19 (6 nm) ^a	3.5×10^{-2}	2.3×10^{-1}

^a Particle size estimated from dispersion data using the formula in Ref. [22].^b TOFs are estimated in the following conditions: $P_{\text{CH}_4} = 0.5$ kPa, $P_{\text{H}_2\text{O}} = 1.1$ kPa, $T = 350$ °C.**Fig. 4.** CH₄ conversion during CH₄-TPR of the fresh and the conditioned 1% Pd/Al₂O₃ (a), 2% Pd/Al₂O₃ (b) and 4% Pd/Al₂O₃ (c).

7–8 nm for the fresh sample and 7 nm for the conditioned-600 one, confirming that no appreciable growth of the PdO crystallites occurred during the conditioning. Besides, the estimated dimensions

**Fig. 5.** XRD spectra of the support and of the oxidized (a) and the reduced in H₂ at 500 °C (b) fresh and conditioned 2% Pd/Al₂O₃ catalysts.

are in good agreement with H₂ chemisorption results, implying that PdO reduction under H₂ at 500 °C does not promote further agglomeration/growth of Pd particles.

Fig. 5b shows the XRD spectra of the fresh (i.e., treated at 600 °C in air) and the conditioned 2% Pd samples upon reduction by H₂ at 500 °C, the same pre-treatment used before H₂ chemisorption and FT-IR analyses. For both the fresh and conditioned catalysts, only metal Pd reflections are visible, in addition to the alumina support patterns, while no PdO peaks are detected. The Pd° crystallites size, estimated on the basis of Scherrer equation, is about 7 nm, a value in line with the Pd dispersion measured by H₂ chemisorption, and did not change before and after the conditioning process, indicating that no crystallite growth occurred.

3.3.2. FT-IR studies

In Fig. 6, the FT-IR spectra of catalysts and support following outgassing at 500 °C are reported in the OH stretching region. The spectrum of the support (Fig. 6, spectrum a) shows the typical band pattern of transitional aluminas characterized by bands at

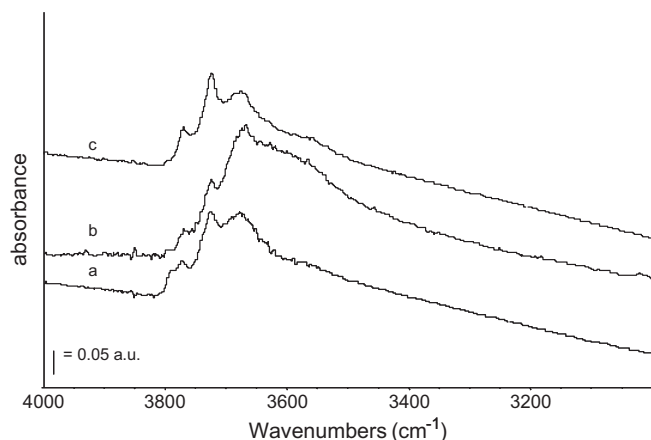


Fig. 6. FT-IR spectra of pure powder samples following outgassing at 500 °C: (a) alumina support, (b) fresh 2% Pd/Al₂O₃, and (c) fully conditioned 2% Pd/Al₂O₃. OH stretching region.

3790 (shoulder), 3770, 3723 cm⁻¹, due to terminal OHs over tetrahedrally coordinated Al ions either in a non-vacant environment or near in a cation vacancy, and to terminal OHs over octahedrally coordinated Al ions. Bands at 3675 and 3570 cm⁻¹ are assigned to bridging and residual triple-bridging hydroxy groups [30]. The IR spectrum of the fresh sample Pd/Al₂O₃ shows the same features, although the components at high frequency, and particularly the band at 3790 cm⁻¹, are significantly reduced (Fig. 6, spectrum b). Moreover, the band assigned to bridging species is broader and tailing toward lower frequencies, probably due to an increased formation of H-bonds among more disordered hydroxy groups. In the conditioned sample spectrum (Fig. 6, spectrum c), isolated OH bands show features very close to the alumina support spectrum, and it is also possible to detect a relative decreasing in intensity of multicoordinated hydroxyl bands, which become slightly less intense than in the pure support spectrum.

FT-IR spectra of CO adsorbed over the fresh catalyst following reduction in hydrogen at 500 °C are reported in Fig. 7.

At CO saturation of the surface (–130 °C), several components appear in the 2300–1700 cm⁻¹ spectral region. A strong band is centered at 2190 cm⁻¹, shifting toward higher frequencies and decreasing in intensity at decreasing CO coverage. The position and behavior of this band allow its assignment to CO coordinated over exposed Al³⁺ ions [31]. Another component at lower frequencies (2160 cm⁻¹), showing the same behavior at decreasing CO coverage, has been previously assigned for supported Pd catalysts to CO coordinated either over Pd²⁺ ions of PdO species or acting as counterions in Pd-containing zeolites, either to physisorbed CO interacting with OH groups of the support [32–34]. The latter assignment is here supported by the spectrum resulting from CO adsorption over pure alumina (Fig. 7, inset) where two components are clearly detectable at 2190 and 2160 cm⁻¹ (shoulder), due to carbonyl over Al ions and to CO interacting with OH groups, respectively. On the other side, we cannot rule out the possibility to have some residual Pd²⁺ ions species at the surface, namely residual PdO particles. At lower frequencies, a complex absorption band can be detected, showing at least three components centered at 2143, 2130 and 2116 cm⁻¹, which behave differently at decreasing CO coverage. The component at 2143 cm⁻¹ disappears almost immediately following outgassing, i.e. just below the complete surface CO saturation, while the other two components are still detectable. According to literature results, the former two bands can be assigned to CO adsorbed over Pd ions (likely Pd²⁺ ions) dispersed at the catalyst surface and strongly interacting with the surface (2143 cm⁻¹) and to CO adsorbed over slightly oxidized Pd^{δ+} species (2130–2125 cm⁻¹) [35]. Following outgassing, the component at 2130 cm⁻¹ decreases in intensity but is still evident at low CO coverages, where bands due to carbonyl over ionic species have already disappeared. Its wavenumber is almost constant, a clear indication of the lacking of lateral interactions, thus isolated species. The complex component just above 2100 cm⁻¹, composed by two maxima at 2116 and 2104 cm⁻¹, is detected as a shoulder

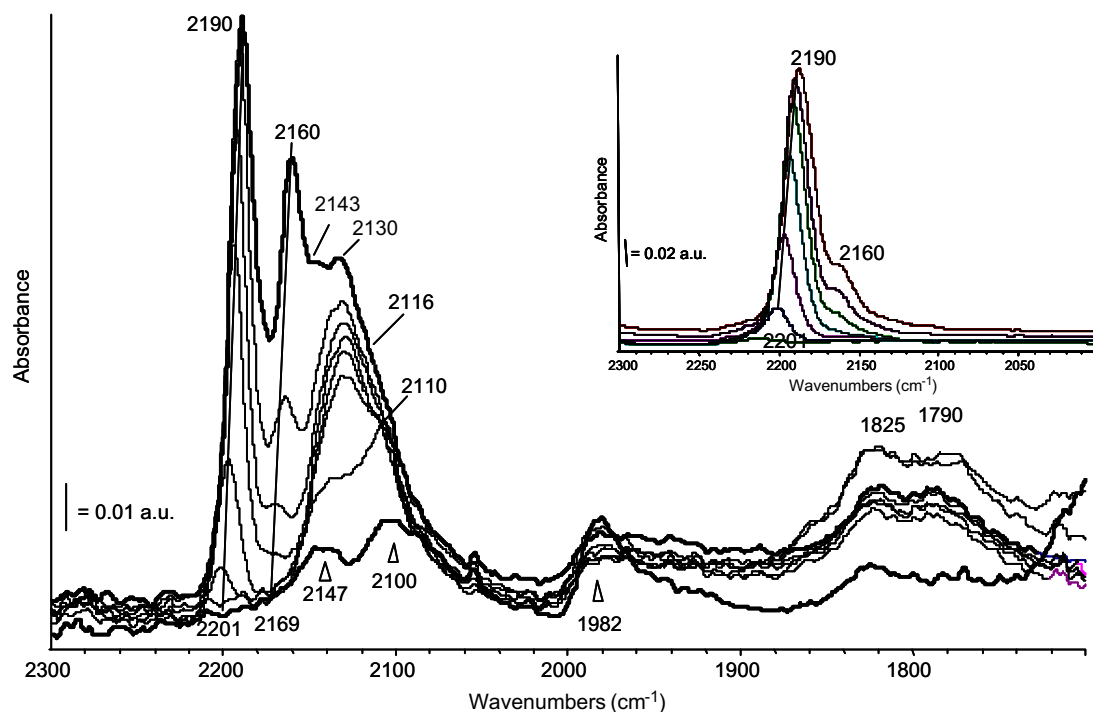


Fig. 7. FT-IR spectra of CO adsorbed over fresh 2% Pd/Al₂O₃ sample following reduction in H₂ at 500 °C and contact with CO at –130 °C. From top to bottom: outgassing upon warming from –130 to 0 °C. The reduced surface spectrum has been subtracted. Inset: CO adsorption over alumina support from –140 °C (high coverage) to 0 °C.

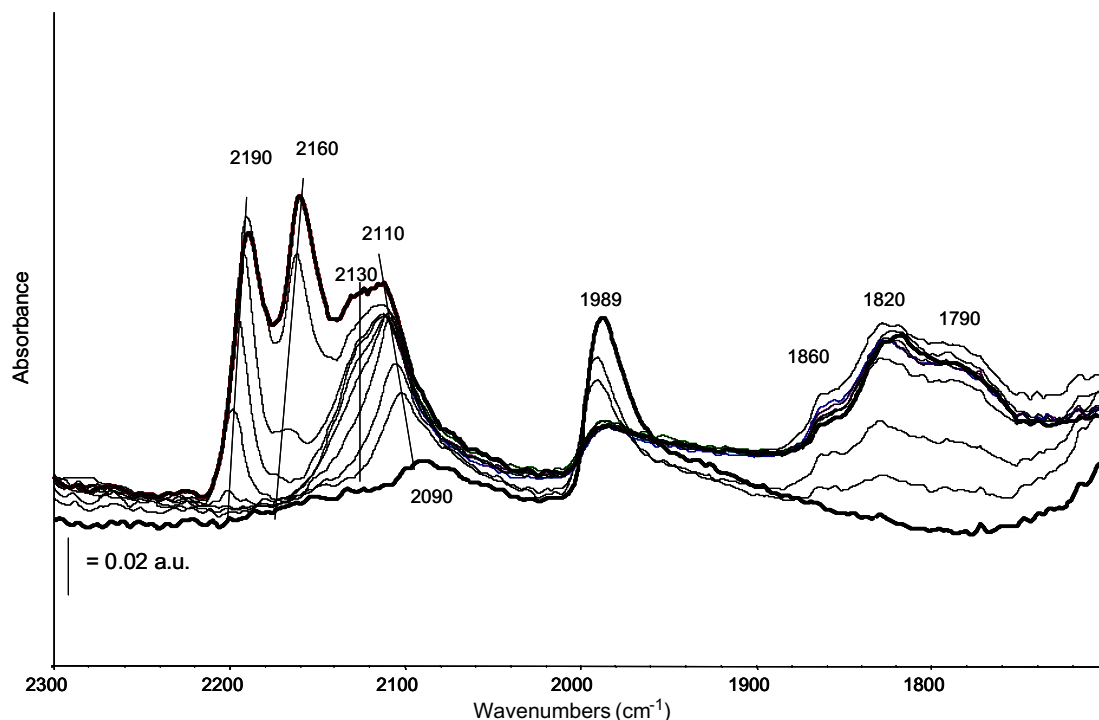


Fig. 8. FT-IR spectra of CO adsorbed over fully conditioned 2% Pd/Al₂O₃ sample following reduction in H₂ at 500 °C and contact with CO at –130 °C. From top to bottom: outgassing upon warming from –130 °C to room temperature. The reduced surface spectrum has been subtracted.

at the highest CO coverage and becomes more clearly defined and centered at 2100 cm^{–1} following outgassing. We assign this band to CO linearly coordinated over metal Pd atoms of low coordination, at particles corner or edge positions. The asymmetric shape of this band, tailing toward lower frequencies, points out the presence of a quite heterogeneous population of Pd metal sites [36–38].

At low CO coverage, the broad band centered at 1980 cm^{–1} becomes the most intense of the overall spectrum (Fig. 7). This feature is due to bridging carbonyls over well-faceted palladium metal particles exposing low index planes and has been assigned to CO bridge bonded over Pd(1 0 0) planes [37,39]. Accordingly, a weak shoulder extending to 1920 cm^{–1} should be assigned to CO twofold coordinated over Pd(1 1 1) planes [9,40]. Finally, threefold bridging carbonyl bands are detected below 1900 cm^{–1}, showing two maxima at 1820 and 1780 cm^{–1}, which can be assigned to threefold bridged carbonyls over Pd(1 1 1) crystal planes [37].

The conditioned catalyst has been reduced in the IR cell following the same procedure applied for the fresh catalyst. FT-IR spectra resulting from low-temperature CO adsorption are reported in Fig. 8. At high CO coverage, the overall spectrum shows two strong bands at 2190 and 2160 cm^{–1}, previously assigned to carbonyl species coordinated over Al ions, residual Pd ions and H-bond CO, respectively. Upon outgassing, these components strongly decrease in intensity and shift toward higher frequencies. The complex band at about 2110 cm^{–1} shows components at 2144, 2130, 2113, 2105 cm^{–1} and below, i.e. almost the same components described for the fresh sample spectra and ascribed to linear carbonyls over partially oxidized Pd (range 2140–2130 cm^{–1}) and over low coordination metallic Pd (range 2110–2090 cm^{–1}), although in this case the relative intensities are significantly changed. In particular, the comparison of the spectra recorded for fresh and conditioned samples at the highest CO coverage (reported in Fig. 9) clearly shows that the complex component at 2110 cm^{–1}, detected as a shoulder in the fresh sample spectra, becomes the main maximum in the conditioned sample spectra. This feature, shifting to 2090 cm^{–1} at decreasing coverage, has been confidently assigned

to CO linearly coordinated over highly dispersed Pd metal particles. Following outgassing up to room temperature, the components due to carbonyl over ionic Pd decrease and completely disappear.

At low coverage, the band at 1989 cm^{–1} due to bridging species on Pd(1 0 0) facets becomes the strongest of the overall spectrum and resists outgassing up to room temperature, in agreement with IR data reported by Primet et al. [9] for alumina-supported Pd catalysts. The complex absorption showing three maxima at 1860, 1820 and 1790 cm^{–1} due to threefold bridging CO likely over both exposed Pd(1 0 0) and (1 1 1) facets is related to the presence of large, well-structured Pd metal particles. The evolution of this component following outgassing to the lowest coverage is quite surprising: the absorption, which is supposed to be the most stable, completely disappears, while the bridging carbonyls are still well evident. This effect could be due to a surface rearrangement,

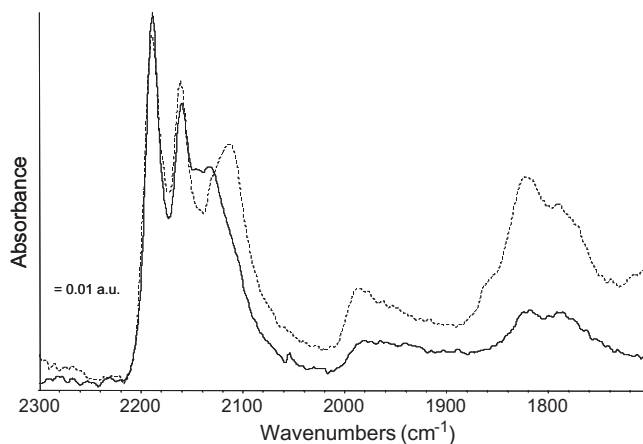


Fig. 9. FT-IR spectra of CO adsorbed over fresh and fully conditioned 2% Pd/Al₂O₃ sample (broken line) following reduction in H₂ at 500 °C and contact with CO at –130 °C. The reduced surface spectrum has been subtracted.

maybe favoring the evolution of threefold species into twofold ones.

4. Discussion

Concentration profiles illustrated in Fig. 1 indicate that in all the investigated catalysts, palladium reversibly undergoes complete reduction during the O₂-free pulses and complete re-oxidation upon restoring lean conditions during the alternated lean combustion/CH₄-reducing pulse at 350 °C. As evidenced by conversion data in Figs. 2 and 3 for all the samples, several Pd reduction/re-oxidation cycles result in a marked (one order of magnitude) activity enhancement and in the achievement of stable performances, which are then reproducible cycle after cycle. A similar phenomenon was also observed for Pd/ZrO₂ catalysts by Bell and co-workers [41] who reported that a series of oxidation and reduction cycles were necessary to obtain a stable methane combustion activity, sixfold higher compared to the initial activity. It was evidenced that no modifications of palladium dispersion occurred along with this activation process. On the other hand, the CH₄-TPR profile changed during the reduction/re-oxidation cycles up to the achievement of a reproducible final profile, characterized by a higher PdO reducibility with respect to the initial one.

Similarly to what reported by Bell and co-workers [41], the comparison of CH₄-TPR profiles of the fresh and the conditioned catalysts shown in Fig. 4 indicates that in all the investigated samples, PdO reducibility increased after the conditioning process, PdO reduces in the conditioned samples starting at temperatures 10–30 °C lower than in the fresh ones. The increase in PdO reducibility under CH₄ may be correlated with the observed increase in catalytic activity, according to Mars–Van Krevelen mechanism controlled by PdO reduction step, i.e. the most accepted mechanism for CH₄ combustion reaction over Pd-based catalysts [9,20,42].

Pd dispersion data in Table 1 indicated that only in the case of the 1% Pd sample, dispersion decreased from 66% for the fresh catalyst to 48% for the conditioned one, while in the case of the 2% and 4% samples, dispersion was constant during the conditioning process. For the 1% Pd sample, the decrease in metal dispersion may be partially responsible for the activity/reducibility increase observed during the conditioning process. An increase in activity with Pd particle size has been widely reported in the literature [3,5,20,22,23], being associated with a lower PdO bond strength in larger particles. Noteworthy, the comparison of TOF values reported in Table 1 evidenced that the more dispersed 1% Pd sample exhibits an intrinsic activity which is one order of magnitude lower than the activity of the less dispersed 2% and 4% Pd samples. On the other hand, in the case of the 2% and 4% Pd catalysts, metal dispersion values of the fresh samples are substantially maintained after the conditioning; thus, for these two samples, a role of Pd dispersion to explain the observed increase in activity/reducibility can be ruled out.

In line with the H₂ chemisorption results, the XRD spectra collected for the fresh and conditioned 2% Pd sample after H₂ reduction at 500 °C, showed in Fig. 5, confirmed that no variations in metallic Pd⁰ crystallites size occurred upon conditioning. The spectra of the unreduced samples indicated the presence of a less crystalline PdO in the conditioned sample than in the fresh one. The reason is the lower temperature of the oxidation treatment (lean reaction conditions at 350 °C) vs. calcination treatment in air at 600 °C used in the preparation of the fresh system, as shown by the comparison of the spectra of the fresh and the conditioned catalysts exposed to dry lean combustion condition at 600 °C (conditioned-600), which are practically identical. To investigate the possibility that the presence of two differently crystallized PdO species might play a major role in determining the differences of activity between the fresh and the conditioned samples, a CH₄ isothermal lean combustion test at 350 °C was performed also over the conditioned-600 sample, under the standard conditions adopted in this study. The conditioned-600 sample exhibited a conversion level of about 60%, a very close value to that obtained with the conditioned sample (70%) and much higher than that observed over the fresh one (10%), thus ruling out the possibility that the differences in catalytic activity between the fresh and the conditioned sample were mainly due to the formation of less crystallized PdO.

For the 2% Pd/Al₂O₃, which is representative of the situation in which Pd dispersion is medium/low (about 20%) and kept constant before and after the alternated cycles treatment, the reason behind the increased activity/reducibility during the conditioning process was further investigated by means of FT-IR spectroscopy. The analysis of the OH stretching region of the spectra reported in Fig. 6 shows that Pd deposition over the unreduced catalyst is related to the disappearance of the high-frequency OH bands, which are associated with Al ions in the tetrahedral environment, thus “basic” hydroxyl groups. These data are in agreement with the results described for alumina-supported Pt by Malpartida et al. [43], suggesting that the location of the smallest Pt particles is selectively substituting or exchanging OH sites on tetrahedral Al ions.

Likely, impregnation of alumina with Pd nitrate solution, thus an acidic metal precursor, affects preferentially the first type of hydroxyls, working as surface germination sites during the impregnation step and the following thermal treatments only partially restored the initial hydroxyl groups of the support. Conditioning leads to the detection of very similar spectral features for the conditioned catalyst and for the support. Thus, strong Pd–support interactions are not weakened after the calcination treatment but only after the conditioning process. This effect can be taken as an evidence of a lowered metal–support interaction consequent to the conditioning.

CO adsorption over fresh 2% Pd/Al₂O₃ reduced in hydrogen at 500 °C allows a detailed analysis of the catalyst surface: the main features from CO low-temperature adsorption are summarized in Table 2. The complexity of bands at frequencies above 2100 cm^{−1}

Table 2
Summary of the main IR features arising from low-temperature CO adsorption over 2%Pd/Al₂O₃ catalyst.

Assignment	Fresh		Fully conditioned	
	High coverage (−130 °C)	Low coverage (outgassing)	High coverage (−130 °C)	Low coverage (outgassing)
Al ³⁺ -CO	2190	2201	2190	2200
CO...HO/Pd ²⁺ -CO	2160	–	2161	2160–2100 vw
Pd ⁿ⁺ -CO	2140	2147	2144 sh	–
Pd ^{δ+} -CO	2133	2134 sh	2129 sh	–
Pd ⁰ -CO	2116–2104 sh	2100	2113–2098	2005
(Pd ⁰) ₂ CO	1980, broad	1982	1985, broad	1989
(Pd ⁰) ₃ CO	1825, 1790	1830	1860, 1820, 1790	–

sh: shoulder; vw: very weak.

is due to the formation of an heterogeneous population of Pd species, characterized by oxidation states ranging from ionic (Pd^{2+}) as in the PdO_x surface “raft” particles to almost metallic ($\text{Pd}^{\delta+}$), i.e. Pd atoms or clusters strongly interacting with the support. The results of these adsorption experiments are in agreement with literature findings for Pd nanoparticles supported over different oxides. Recently, Schalow et al. [44] proposed the existence of “surface oxide” particles formed following the oxidation of Pd metal nanoparticles below 500 K and characterized by peaks at 2133 and 1960 cm^{-1} in IRAS spectra of adsorbed CO. The nature of these particles has been reported as mainly metallic, on which metallic surface areas and surface oxides co-exist. Skotak et al. reported the detection of bands at $2135\text{--}2138\text{ cm}^{-1}$ in the spectra of CO adsorbed over Pd/alumina system, regardless of CO coverage, associated with Pd^+ in the alumina matrix [45,46].

As for the metal particles, characterized by on-top, bridging and triple-bridging carbonyl species, the spectra observed for carbonyls on reduced fresh catalyst are fully consistent with those reported by several authors for reduced $\text{Pd}/\text{Al}_2\text{O}_3$ catalysts [34,36,37, 43,44]. In particular, the high frequency of the on-top CO band is in agreement with its assignation to CO coordinated over corner, edges and low-coordination sites of Pd metal surface, and its broad shape indicates an heterogeneity of the metal particles, consistent both with the presence of (1 1 1) and (1 0 0) crystal planes [34]. The interpretation of the IR data, coupled with H_2 chemisorption results, suggests that large particles are present together with smaller ones, as deduced by the intensity and complexity of the bands of bridging and triple-bridging CO. The position of these bands is a further evidence of large metal particles exposing Pd(1 1 1) and Pd(1 0 0) planes.

To some extent, the spectra of CO adsorption recorded at low temperature and high CO coverage over the conditioned catalyst surface show roughly similar features in the spectral regions $2190\text{--}2110$ (carbonyls on ionic and slightly oxidized Pd species) and $2100\text{--}1790\text{ cm}^{-1}$ (carbonyls on metal Pd). However, a closer comparison of the spectra obtained at low temperature, in a condition which approaches the full CO coverage of the surface, evidenced the following differences (Fig. 9). As for the ionic species, carbonyls adsorbed on dispersed PdO_x species and Pd ions strongly interacting with the support, clearly detected over the fresh sample, are significantly reduced, while terminal carbonyl over zerovalent Pd particles are predominant in the conditioned sample spectra, the component at 2130 cm^{-1} becoming here just a shoulder of the stronger 2110 cm^{-1} band. This effect can be explained considering that for the conditioned sample, the fraction of species strongly interacting with the surface is reduced with respect to the fresh one in favor of low-coordination Pd metal particles. This is another evidence that conditioning process resulted in the weakening of the interactions between palladium and the alumina support, which stabilizes the oxidized palladium species against reduction, thus penalizing catalytic activity of the fresh samples.

Although FT-IR spectra were collected only in the case of the reference 2% $\text{Pd}/\text{Al}_2\text{O}_3$ sample, it is likely that the weakening of palladium–support interactions during the conditioning process occurs also in the case of the 4% Pd catalyst, which exhibits a very similar behavior, i.e. an increase in activity–reducibility not accompanied with modifications of Pd particle size. In the case of the 1% Pd sample, the contribution of the weakening of palladium–support interactions in the activation process is likely combined with the contribution of Pd dispersion modifications. The very high dispersion value of the fresh sample, which cannot be maintained under operating conditions, leads to stronger Pd–support interactions, which may make weakening more difficult, thus determining the slow conditioning process observed for the 1% Pd catalyst.

5. Conclusions

The main conclusions obtained in this work can be summarized in the following points:

1. A conditioning process of $\text{Pd}/\text{Al}_2\text{O}_3$ catalysts consisting of several cycles of alternated CH_4 lean combustion/ CH_4 -reducing pulses at $350\text{ }^\circ\text{C}$ resulted in a marked increase in catalytic activity cycle after cycle, up to a stable final level, about one order of magnitude higher than the initial one. For each catalyst, the activation is correlated with the increase in PdO reducibility as observed in CH_4 -TPR experiments, in line with the Mars–Van Krevelen mechanism controlled by the PdO reduction step proposed in the literature.
2. Only slight modifications of Pd dispersion upon the conditioning process occurred on the 1% Pd sample, while no changes occurred in the 2% and 4% Pd catalysts. Accordingly, a significant role of variations in Pd particle size can be excluded.
3. The FT-IR spectra following outgassing at $500\text{ }^\circ\text{C}$ evidenced that the high-frequency hydroxyls groups of alumina are strongly reduced in intensity over the fresh sample, suggesting that impregnation of the support with the acid Pd precursor solution titrates the basic hydroxyls groups, leading to strong metal–support interactions: these interactions are not removed by the calcination treatment but they are weakened during the conditioning process, as suggested by the spectra of the conditioned sample which exhibits features in the OH stretching region very similar to those of the alumina.
4. CO adsorption collected for the 2% $\text{Pd}/\text{Al}_2\text{O}_3$ catalyst evidenced a clear reduction in the band assigned to the slightly oxidized Pd (2130 cm^{-1}), strongly interacting with the surface, in the conditioned sample with respect to the same fresh one; this confirms that during the conditioning, Pd–support interactions, which likely stabilize the oxidized Pd species against reduction, are weakened and this is likely responsible for the marked enhancement of catalytic activity.

References

- [1] P. Gelin, M. Primet, *Applied Catalysis B: Environmental* 39 (2002) 1–37.
- [2] B.Y. Chin, D.E. Resasco, *Catalysis* 14 (1999) 1–39.
- [3] P. Castellazzi, G. Groppi, P. Forzatti, A. Baylet, P. Marecot, D. Duprez, *Catalysis Today* 155 (2010) 18–26.
- [4] D. Ciuparu, M.R. Liubovsky, E. Altmann, L.D. Pfefferle, A.D. Datye, *Catalysis Review* 44 (2002) 591.
- [5] R.F. Hicks, H. Qi, M. Young, R. Lee, *Journal of Catalysis* 122 (1990) 280.
- [6] T.R. Baldwin, R. Burch, *Applied Catalysis* 66 (1990) 337–358.
- [7] P. Briot, M. Primet, *Applied Catalysis* 69 (1991) 301–314.
- [8] N. Mouaddib, C. Feumi-Jantou, E. Garbowski, M. Primet, *Applied Catalysis A: General* (1992) 129.
- [9] E. Garbowski, C. Feumi-Jantou, N. Mounaddib, M. Primet, *Applied Catalysis A: General* 109 (1994) 277–291.
- [10] T.R. Baldwin, R. Burch, *Catalysis Letters* 6 (1990) 131.
- [11] L.P. Haack, K. Otto, *Catalysis Letters* 34 (1995) 31.
- [12] D. König, W.H. Weber, B.D. Poindexter, J.R. McBride, J.W. Graham, K. Otto, *Catalysis Letters* 29 (1994) 329.
- [13] K. Otto, C.P. Hubbard, W.H. Weber, G.W. Graham, *Applied Catalysis B: Environmental* 1 (1992) 317.
- [14] D. Roth, P. Gelin, M. Primet, E. Tena, *Applied Catalysis A* 203 (2000) 37–45.
- [15] R. Burch, *Pure and Applied Chemistry* 68 (1996) 377.
- [16] R. Burch, *Catalysis Today* 35 (1997) 27–36.
- [17] C.F. Cullis, B.M. Willat, *Journal of Catalysis* 86 (1984) 187–200.
- [18] R.S. Monteiro, D. Zemlyanov, J.M. Storey, F.H. Ribeiro, *Journal of Catalysis* 199 (2001) 291.
- [19] R.S. Monteiro, D. Zemlyanov, J.M. Storey, F.H. Ribeiro, *Journal of Catalysis* 201 (2001) 37–45.
- [20] C.A. Müller, M. Maciejewski, R.A. Koeppel, A. Baiker, *Journal of Catalysis* 166 (1997) 36.
- [21] F.H. Ribeiro, M. Chow, R.A. Dalla Betta, *Journal of Catalysis* 146 (1994) 537.
- [22] D. Roth, P. Gelin, A. Kaddouri, E. Garbowski, M. Primet, E. Tena, *Catalysis Today* 112 (2006) 134.
- [23] K. Fujimoto, F.H. Ribeiro, M. Avalos-Borja, E. Iglesia, *Journal of Catalysis* 179 (1998) 431–442.

- [24] G. Zhu, J. Han, D.Y. Zemlyanov, F.H. Ribeiro, *Journal of American Chemical Society* 126 (2004) 9896–9897.
- [25] S.C. Su, J.N. Carstens, A.T. Bell, *Journal of Catalysis* 176 (1998) 125.
- [26] F. Arosio, S. Colussi, A. Trovarelli, G. Groppi, *Applied Catalysis B: Environmental* 80 (2008) 335–342.
- [27] C.F. Cullis, B.M. Willat, *Journal of Catalysis* 83 (1983) 267.
- [28] Y.Y. Yao, *Industrial and Engineering Chemistry Product Research and Design* 19 (1980) 293.
- [29] K. Fujimoto, F.H. Ribeiro, A.T. Bell, E. Iglesia, *ACS Division of Petroleum Chemistry Preparation* 41 (1996) 110.
- [30] G. Busca, *Chemical Reviews* 107 (2007) 5366–5410.
- [31] K.I. Hadjiivanov, G.N. Vayssilov, *Advances in Catalysis* 47 (2002) 308.
- [32] P. Gelin, A.R. Siedle, J.T. Yates Jr., *Journal of Physical Chemistry* 88 (1984) 2978–2985.
- [33] D. Scarano, S. Bordiga, C. Lamberti, G. Ricchiardi, S. Bertarione, G. Spoto, *Applied Catalysis A: General* 307 (2006) 3–12.
- [34] S. Specchia, E. Finocchio, G. Busca, P. Palmisano, V. Specchia, *Journal of Catalysis* 263 (2009) 134–145.
- [35] M. Benkhaled, S. Morin, Ch. Pichon, C. Tomazeau, C. Verdon, D. Uzio, *Applied Catalysis A: General* 312 (2006) 1–11.
- [36] S. Bertarione, D. Scarano, A. Zecchina, V. Johanek, J. Hoffmann, S. Schauer mann, M.M. Frank, J. Libuda, G. Rupprechter, H.-J. Freund, *Journal of Physical Chemistry B* 108 (2004) 3603–3613.
- [37] T. Lear, R. Marshall, J.A. Lopez-Sanchez, D.D. Jackson, T.M. Klapotke, M. Baumer, G. Rupprechter, H.-J. Freund, D. Lennon, *Journal of Chemical Physics* 123 (2005) 174706.
- [38] G. Agostini, R. Pellegrini, G. Leofanti, L. Bertinetti, S. Bertarione, E. Groppo, A. Zecchina, C. Lamberti, *Journal of Physical Chemistry C* 113 (2009) 10485–10492.
- [39] F. Di Gregorio, L. Bisson, T. Armadori, C. Verdon, L. Lemaitre, C. Thomazeau, *Applied Catalysis A: General* 352 (2009) 50–60.
- [40] E. Groppo, S. Bertarione, F. Rotunno, G. Agostini, D. Scarano, R. Pellegrini, G. Leofanti, A. Zecchina, C. Lamberti, *Journal of Physical Chemistry C* 111 (2007) 7021–7028.
- [41] J.N. Carstens, S.C. Su, A.T. Bell, *Journal of Catalysis* 176 (1998) 136–142.
- [42] R. Burch, F.J. Urbano, *Applied Catalysis A: General* 124 (1995) 121.
- [43] I. Malpartida, M.A. Larrubia Vargas, L.J. Alemany, E. Finocchio, G. Busca, *Applied Catalysis B: Environmental* 80 (3–4) (2008) 214–225.
- [44] T. Schalow, B. Brandt, M. Laurin, S. Schauer mann, S. Guimond, H. Kuhlbeck, J. Libuda, H.-J. Freund, *Surface Science* 600 (2006) 2528–2542.
- [45] M. Skotak, Z. Karpinski, W. Juszczuk, J. Pielaszek, L. Kepinski, D.V. Kazachkin, V.I. Kovalchuk, J.L. d'Itri, *Journal of Catalysis* 227 (2004) 11–25.
- [46] T. Dellwig, J. Hartmann, J. Libuda, I. Meusel, G. Rupprechter, H. Unterhalt, H.-J. Freund, *Journal of Molecular Catalysis A: Chemistry* 162 (2000) 51.